

HSP60 as one of the player in atherogenic remodeling of thoracic aorta in photoperiod induced chronodisruption

Introduction

The development of atherosclerosis is believed to be primarily associated with hyperlipidemia. However, most of the patients have been reported to have levels of cholesterol within the normal range, suggesting that high blood cholesterol is not the only most important risk factor for atherosclerosis (Fernandez-Friera et al., 2017; Ridker et al., 2008; Sniderman et al., 1980). It further implies towards a pathophysiology that is independent of blood cholesterol levels, at least for atherogenic initiation. Abnormal expression of HSP60 in stressed endothelium has emerged as a plausible explanation for atherosclerotic lesion developed in normolipidemic conditions (Wick et al., 2014). In this regard, evidences have been documented from two cross-sectional clinical studies in young volunteers. In these studies, clinically healthy young men and women showed intima-media thickening that correlated significantly with T cell reactivity against HSP60. Active and passive smoking were identified as the most important risk factor for atherosclerosis in these cohorts (Knoflach et al., 2003; Knoflach et al., 2009). Another study with human subjects showed early atherosclerotic lesions that harbored HSP60-specific T cells and endothelial HSP60 overexpression wherein, hypertension and smoking has been found to be the associated risk factors in subjects with normolipidemic status (Almanzar et al., 2012). Further, *in vitro* and *in vivo* studies had shown ectopic HSP60 expression in vascular endothelium on exposure to a variety of known atherogenic stressors including LPS, pro-inflammatory cytokines, Chlamydial infections, fluid shear stress, smoking, hypertension and hyperlipidemia (Amberger et al., 1997; Hochleitner et al., 2000; Jakic et al., 2017;

Kreutmayer et al., 2011; Kreutmayer et al., 2013; Seitz et al., 1996). Thus, upregulation of HSP60 in the vascular wall has been recognized as a central mediator of atherogenic initiation, even in conditions of normolipidemia.

Accumulating evidences have implied to a strong association of biological rhythm disruption with atherogenic manifestations. Intrinsic circadian clock of the body is known to regulate synchrony of physiological processes and the mechanism involves a close coordination between the central clock situated in the supra-chiasmatic nuclei of the hypothalamus and the peripheral oscillators in tissues and organs. The regulatory mechanisms are defined by the transcriptional-translation feedback loops with Bmal1 and Clock as the central transcription factors. Any change in the normal light-dark cycle leads to impairment of the core clock machinery that can have profound consequences on health (Albrecht, 2012).

With the technological advancement and the associated industrial revolution, there has been constant changes in the working shifts of people. Further, an increment in the social pressure directly relates with widespread use of artificial light and electronic gadgets that results in chronic disruption of the biological rhythm (Figueiro, 2017). Also, frequent long distance travel across multiple time zones lead to a disturbance of the intrinsic circadian rhythm (Vosko, 2010). Regardless of the source, dysregulated circadian rhythm has clearly been demonstrated to be the underlying cause of metabolic disorders including cardiovascular diseases. Within this framework, studies have demonstrated that shift workers comprise of a higher risk group for cardiovascular manifestations (Hermansson et al., 2019; Scheer et al., 2009). The records of a cross-sectional study in night shift workers showed that increased arterial stiffness, the earliest pro-atherogenic change, is associated

with shift work (Jankowiak et al., 2016). Cardiovascular mortality has also been observed in factory workers with photoperiodic shifts (Knutsson et al., 2004).

Earlier clinical studies had shown that acute cardiovascular events follow diurnal pattern indicating involvement of circadian clock components (Muller et al., 1985; Willich, 1990). In this regard, deletion or mutation of various circadian genes in murine models of atherosclerosis had been observed to promote plaque formation (Anea et al., 2009; Somanath et al., 2011). Western diet induced lesion formation in aortic root was reported to be aggravated in ApoE*3-Leiden.CETP mice subjected to alternating light dark conditions (Schilperoort et al., 2020). Thus, circadian disruption is an addition to the risk factors for atherosclerosis. Because of its multifactorial nature, the pathogenic mechanism underlying the atherogenic initiation need absolute clarity but till date, many facets remain unexplored. As of now, the experimental evidences in this context have been accumulated from studies with LDLR^{-/-} or ApoE^{-/-} mice models that are genetically hyperlipidemic and hence, these studies do not reflect the sole effects of photoperiodic misalignment in itself.

In the present study, we have assessed the pro-atherogenic vascular changes in thoracic aorta of C57BL/6J mice subjected to photoperiodic manipulation induced chronodisruption (PMCD) for 16 week. A comparative analysis was done with mice fed with high fat high fructose (HFHF) diet for 16 weeks that refers to the hyperlipidemia induced model for atherosclerosis. A combination of HFHF+PMCD has also been put to scientific scrutiny to assess the possible synergistic effect on atherogenic transformation. Status of HSP60 as the possible cause for pro-atherogenic changes in a normolipidemic condition is also investigated herein.

Materials and methods

Experimental model: C57BL/6J male mice aged 4-6 weeks each weighing 20-22g. Particulars of animal maintenance and the ethical statement are provided in Materials and methods section.

Animal Experimentation Protocol

Experimental groups:

After 10 days acclimatization, the mice were randomly divided into four experimental groups as follows:

1. Control group (n=6, fed with standard chow and subjected to normal 12:12 light/dark cycle),
2. HFHF group (n = 10, fed with high fat diet containing 35.3% fat content and 20% fructose in water and subjected to normal 12:12 light dark cycle),
3. Photoperiodic manipulation induced chronodisruption (PMCD) group (n=10, fed with standard chow and subjected to PMCD) and
4. HFHF+PMCD group (n=10, fed with HFHF and subjected to PMCD).

The experimental protocol was carried out for a period of 16 weeks and food intake and body weight was monitored every alternate day. After 16 weeks, mice were euthanized under mild isoflurane anesthesia and blood and thoracic aorta were collected as mentioned in Materials and methods section.

Photoperiodic manipulation induced chronodisruption (PMCD):

The photoperiodic manipulation was carried out using protocol by (Kettner et al., 2015) with minor modifications. Briefly, mice were subjected PMCD by transferring them

between two rooms, Room 1 and Room 2 that were identical in every aspect, except for the light-dark cycle. Room 1 was setup with 7:00 h to 19:00 h light/19:00 h to 7:00 h dark period and Room 2 with 11:00 h to 23:00 h dark/23:00 h to 11:00 h light period. Thus, shifting mice from Room 1 to Room 2 on Monday resulted in phase advance of 8 h (lights off at ZT4) and transferring them back to Room 1 on Thursday resulted in a phase delay of 8 h (lights off at ZT20) (Fig. 4.1). All the transfer of mice between the two rooms was carried out at 10:55 h.

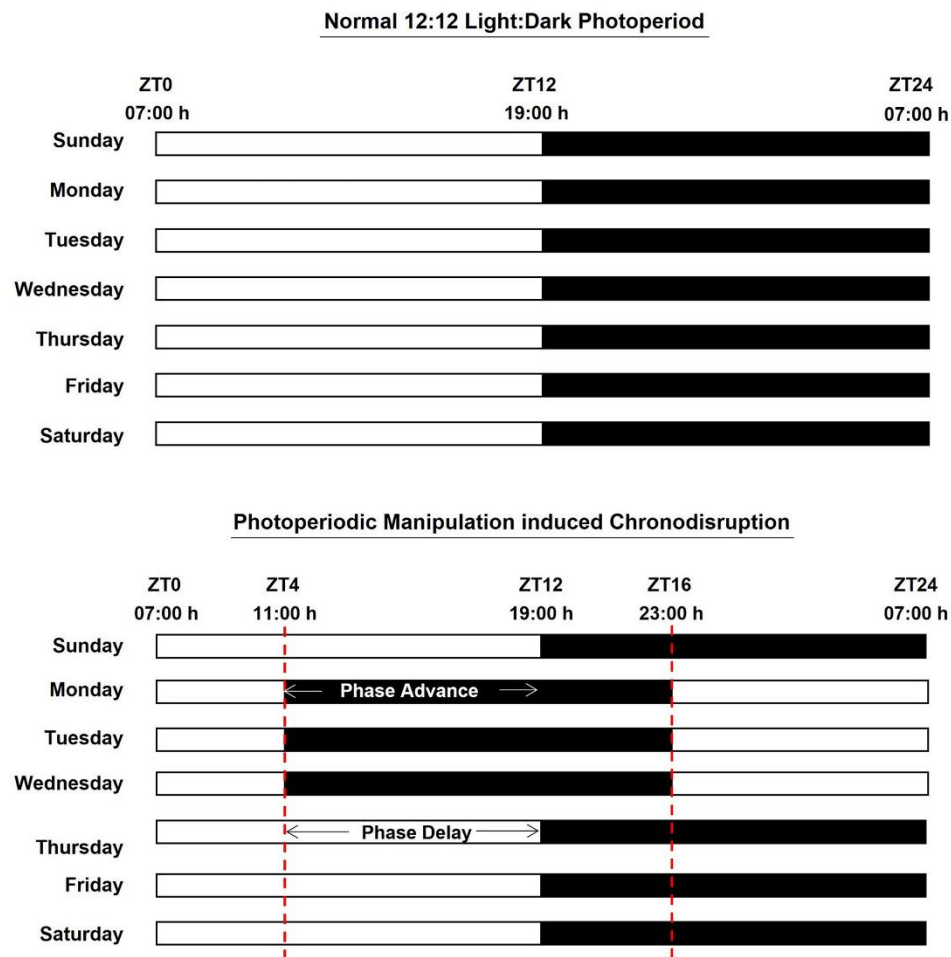


Figure 4.1: Schematic representation of normal and altered photoperiodic regime followed in the study.

Parameters tested:

1. Serum lipid profile: TG, TC, VLDL, LDL-Chol, HDL-Chol, LDL-Chol:HDL-Chol ratio
2. Histology and morphometry
3. Elastin autofluorescence
4. Picrosirius red staining
5. Quantitative RT-PCR: HSP60, Collagen-I, Collagen-II, eNOS, VCAM-1, ICAM-1, MCP-1, HSP10, GAPDH
6. Immunoblotting: HSP60, HSP10, β -actin
7. Immunohistochemistry: HSP60, CD68

The experimental protocol for the present study is depicted in Fig. 4.2. Detailed methodology is described in materials and methods section.

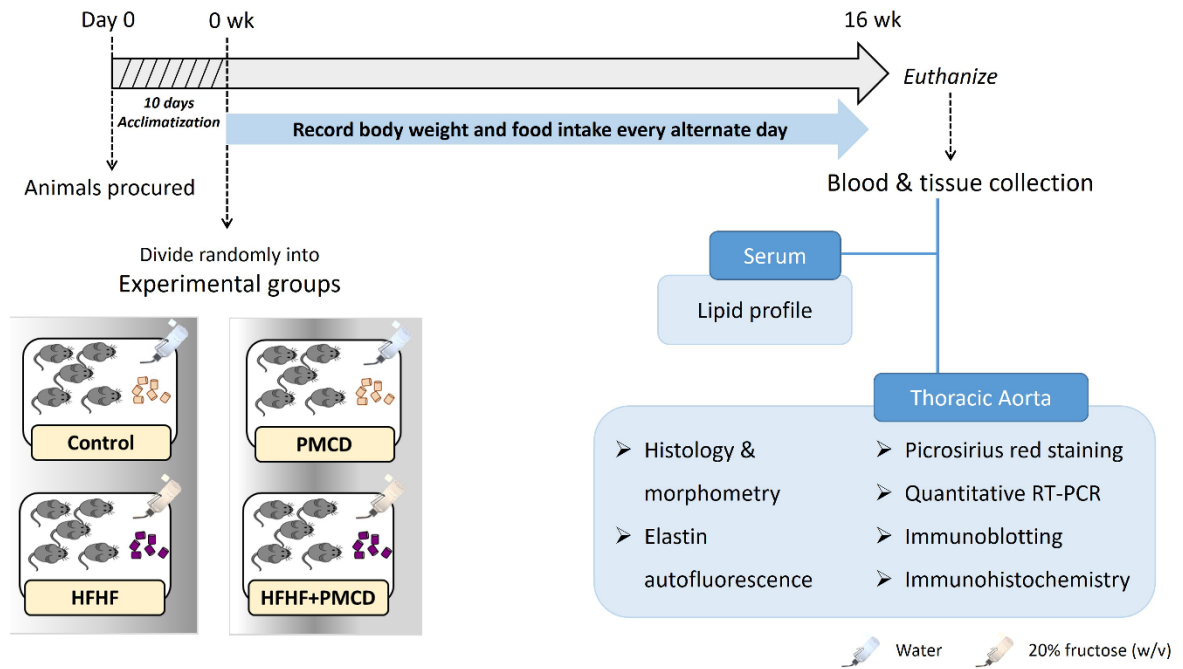


Figure 4.2: Flow chart of the experimental protocol followed for studying chronodisruption induced atherosclerosis.

Results

HFHF and PMCD mediated alterations in food intake and body weight

A significant increment in body weight and decrement in food intake was recorded in HFHF group as compared to control. On the contrary, PMCD group recorded reciprocal set of changes in the said parameters with values comparable to that of control. However, HFHF+PMCD group recorded increment in body weight and decrement in food intake that was comparable to HFHF group (Fig. 4.3).

HFHF and PMCD mediated changes in serum lipid profile

Serum levels of TG, TC, VLDL, LDL-Chol and LDL-Chol:HDL-Chol ratio were significantly elevated in HFHF and HFHF+PMCD groups as compared to Control. PMCD group showed significantly higher levels of TG, VLDL and LDL-Chol: HDL-Chol ratio whereas, a marked decrement in HDL-Chol levels were recorded in all three experimental groups with most significant decrement in PMCD group (Fig. 4.4).

HFHF and PMCD induced vascular remodeling in thoracic aorta

Structural remodeling in intima and media regions of thoracic aorta were observed in HXE stained sections of all the three experimental groups but, the changes were most prominent in PMCD group (Fig. 4.5a). Likewise, all the three groups showed significant increment in intima-media thickness (IMT) with maximal value recorded in PMCD group (Fig. 4.5b). Lumen area showed moderate increment in HFHF and HFHF+PMCD groups as compared to control whereas, PMCD groups recorded significant increment in the same (Fig. 4.5c). Further, microscopic evaluation of autofluorescent sections revealed marked derangement of elastin lamellae in all the three groups with severe effects in PMCD group (Fig. 4.6a). These structural changes were accompanied by significantly higher number of elastin

breaks in all the three experimental groups with highest value recorded in PMCD group (Fig. 4.6b). Similarly, picrosirius red stained sections of thoracic aorta revealed marked thickening of outer collagen along with significant increment in collagen content in all the three groups compared to control (Fig. 4.7a & b). mRNA levels of collagen I were significantly higher in all the three groups compared to control but, only PMCD group recorded a simultaneous upregulation of collagen III mRNA (Fig. 4.7c). The experimental groups also recorded significant increment in collagen-to-elastic ratio (Fig. 4.7d).

HFHF and PMCD induced endothelial dysfunction and activation in thoracic aorta

eNOS mRNA expression was assessed in thoracic aorta as a marker of endothelial function and we observed a moderate decrement (non-significant) in the same in HFHF group. A significant downregulation of eNOS mRNA expression was observed in PMCD and HFHF+PMCD groups (Fig. 4.8a). Further, MCP-1, VCAM-1 and ICAM-1 mRNA expression was checked in thoracic aorta as an indication of endothelial activation. The said markers were significantly upregulated in the three experimental groups compared to control (Fig. 4.8b-d). The subsequent recruitment of macrophages was analyzed by immunolocalization of CD68 (macrophage marker) that was found to be significantly elevated in HFHF, PMCD and HFHF+PMCD groups as evidenced by prominent positive staining of thoracic aorta (Fig. 4.9a & b).

HFHF and PMCD upregulated HSP60 in thoracic aorta

Immunostaining of sections of thoracic aorta with HSP60 showed prominent positively stained regions in HFHF, PMCD and HFHF+PMCD groups as compared to control (Fig. 4.10a). Quantitative analysis of these sections were also found to be significant (Fig.

4.10b). Further, immunoblots of HSP60 in thoracic aorta of the said groups showed similar trend of increment that complimented observations of immunostaining (Fig. 4.10c).

HFHF and PMCD upregulated HSP10 in thoracic aorta

mRNA and protein expression of HSP10 was moderately higher in HFHF and HFHF+PMCD groups whereas PMCD group recorded a significantly elevated levels compared to control (Fig. 4.11 a &b).

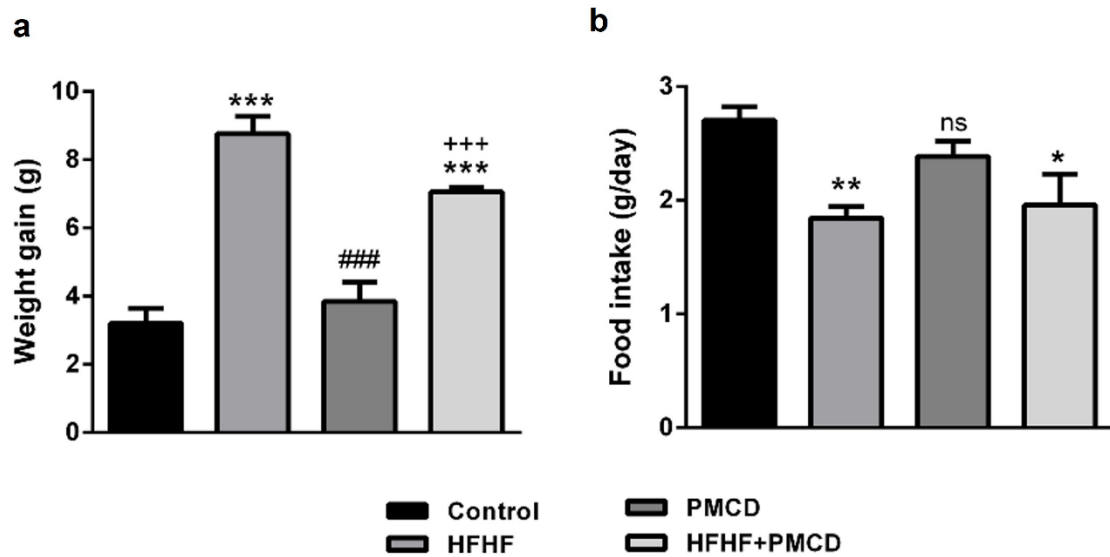


Figure 4.3: Weight gain and food intake in mice. The graphs represent (a) final weight gain per mice and (b) average food intake per mice per day in mice fed with HFHF &/or subjected to PMCD (n=6 for control, n=10 for experimental groups). Data were represented as Mean \pm SEM. *P<0.05, **p<0.01, ***p<0.001 vs Control; ###p<0.001 vs HFHF; +++p<0.001 vs PMCD, ns- non-significant.

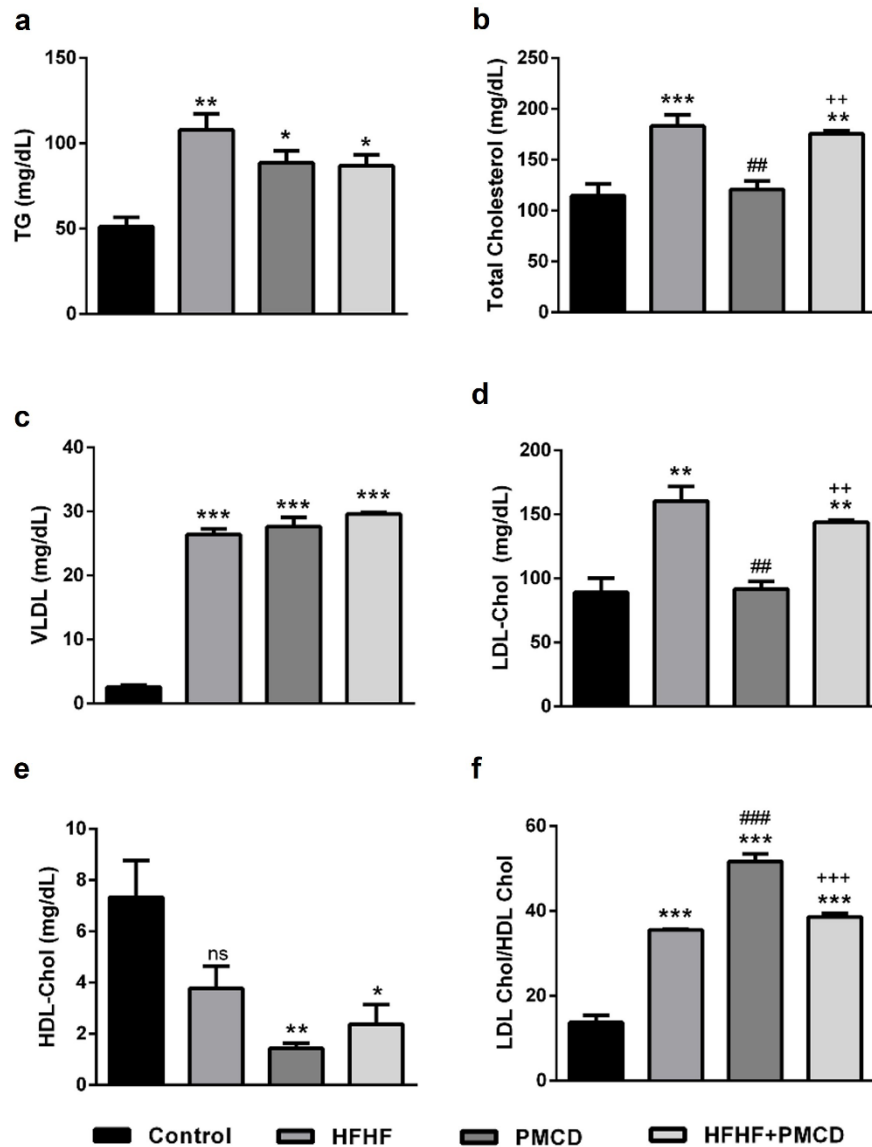


Figure 4.4: Serum lipid profile of mice. The graphs represent serum titers of (a) triglycerides (TG), (b) total cholesterol (TC), (c) very low density lipoprotein (VLDL), (d) low density lipoprotein cholesterol (LDL-Chol), (e) high density lipoprotein cholesterol (HDL-Chol) and (f) LDL-Chol/HDL-Chol ratio were assayed (n=6). Data were represented as Mean \pm SEM. * p <0.05, ** p <0.01, *** p <0.001 vs Control; ## p <0.01, ### p <0.001 vs HFHF; ++ p <0.001, +++ p <0.001 vs PMCD, ns- non-significant.

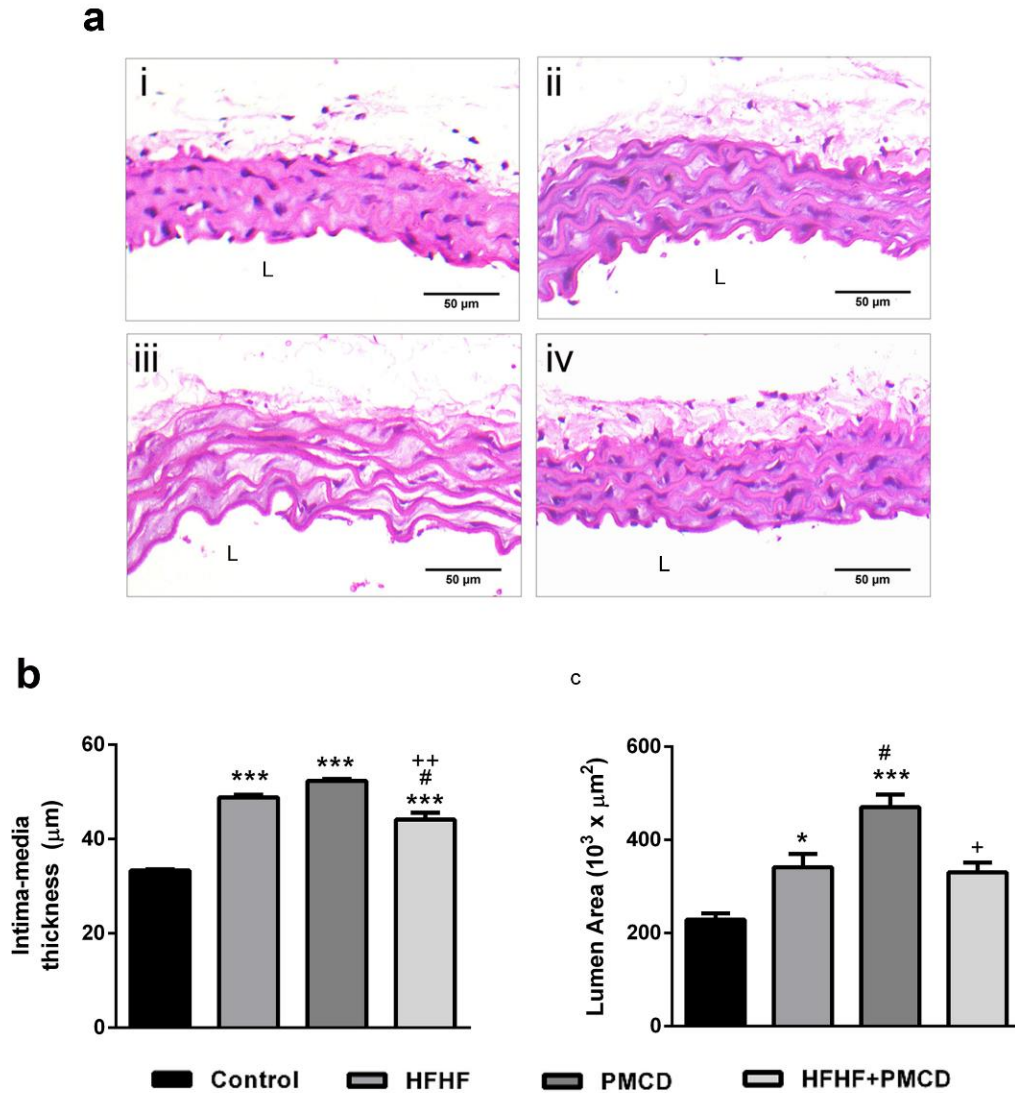


Figure 4.5: Histology and morphometric analysis of thoracic aorta. Sections of thoracic aorta were stained with H&E and (a) representative images of i- Control, ii- HFHF, iii- PMCD, iv- HFHF+PMCD groups are shown (Scale bar= 100μm). Images were used for quantitative assessment of (b) intima-media thickness (IMT) and (c) lumen area (n=6). Data were represented as Mean ± SEM. *p<0.05, ***p<0.001 vs Control; #p<0.05 vs HFHF; +p<0.05, ++p<0.01 vs PMCD, ns- non-significant. L- Lumen.

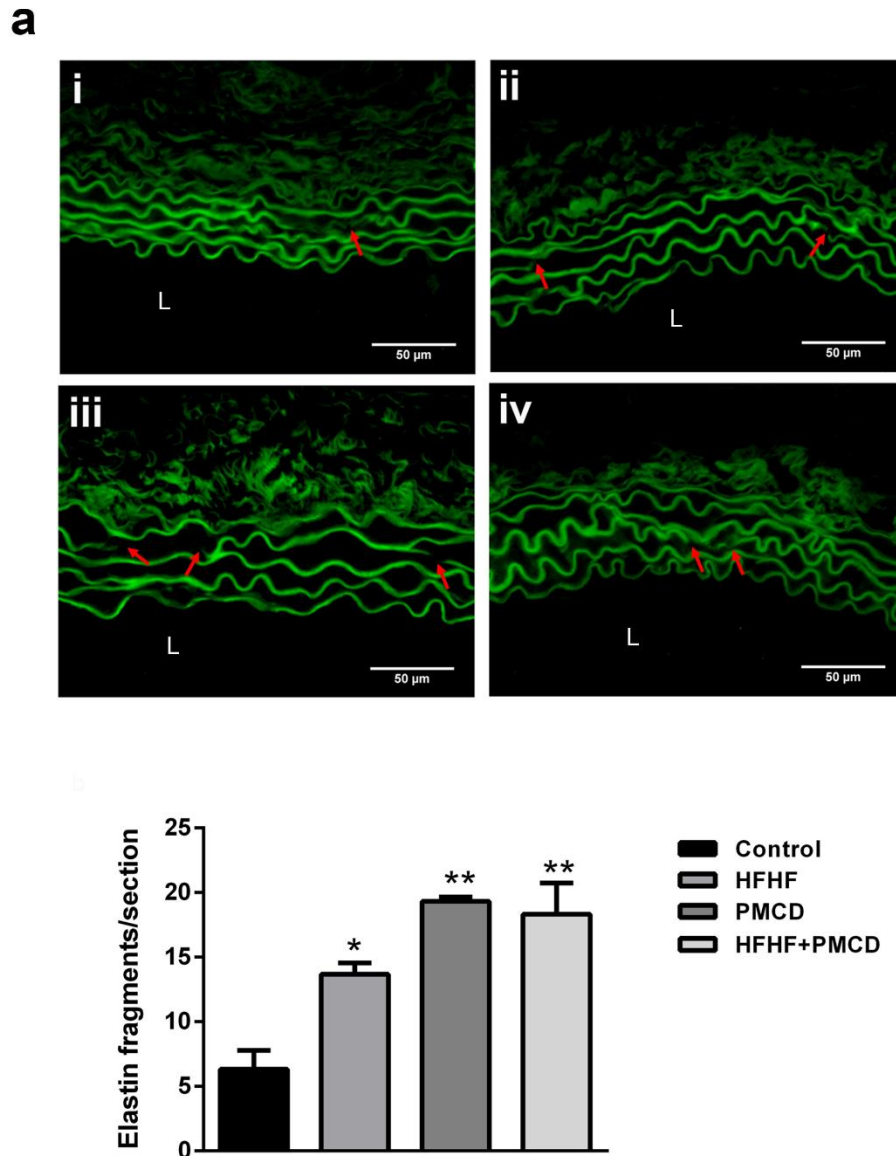


Figure 4.6: Elastin autofluorescence in thoracic aorta. (a) Elastin derangement was assessed in autofluorescent sections of thoracic aorta of i- Control, ii- HFHF, iii- PMCD, iv-HFHF+PMCD groups (scale bar= 100 μ m) where red arrows indicate elastin breaks. (b) Graph represents elastin fragmentation counted from the sections (n=6). Data were represented as Mean \pm SEM. * p <0.05, ** p <0.01 vs Control. Red arrows-elastin breaks, L-Lumen.

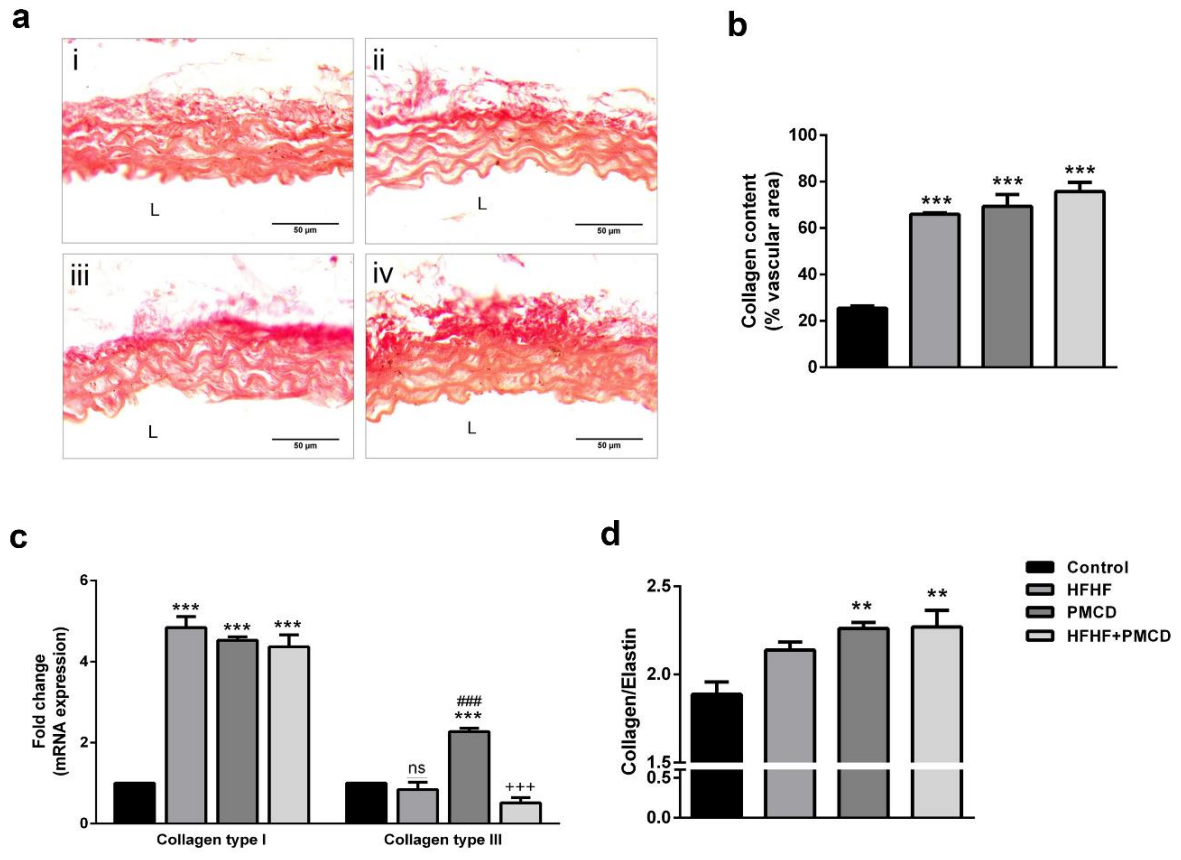


Figure 4.7: Collagen content in thoracic aorta. Sections of thoracic aorta were stained with picrosirius red and (a) images of i- Control, ii- HFHF, iii- PMCD, iv- HFHF+PMCD groups were captured (Scale bar= 50 μ m). Quantitative measurement of (b) collagen content was carried out relative to the vascular area (n=6). (c) mRNA expression of collagen I and collagen III were assessed in thoracic aorta by quantitative RT-PCR (n=3). (d) Collagen-to-elastin ratio (n=6) was quantified from picrosirius red stained sections as a measure of arterial stiffness. Data were represented as Mean \pm SEM. **p<0.01, ***p<0.001 vs Control; ###p<0.001 vs HFHF; +++p<0.001 vs PMCD, ns- non-significant. L- Lumen.

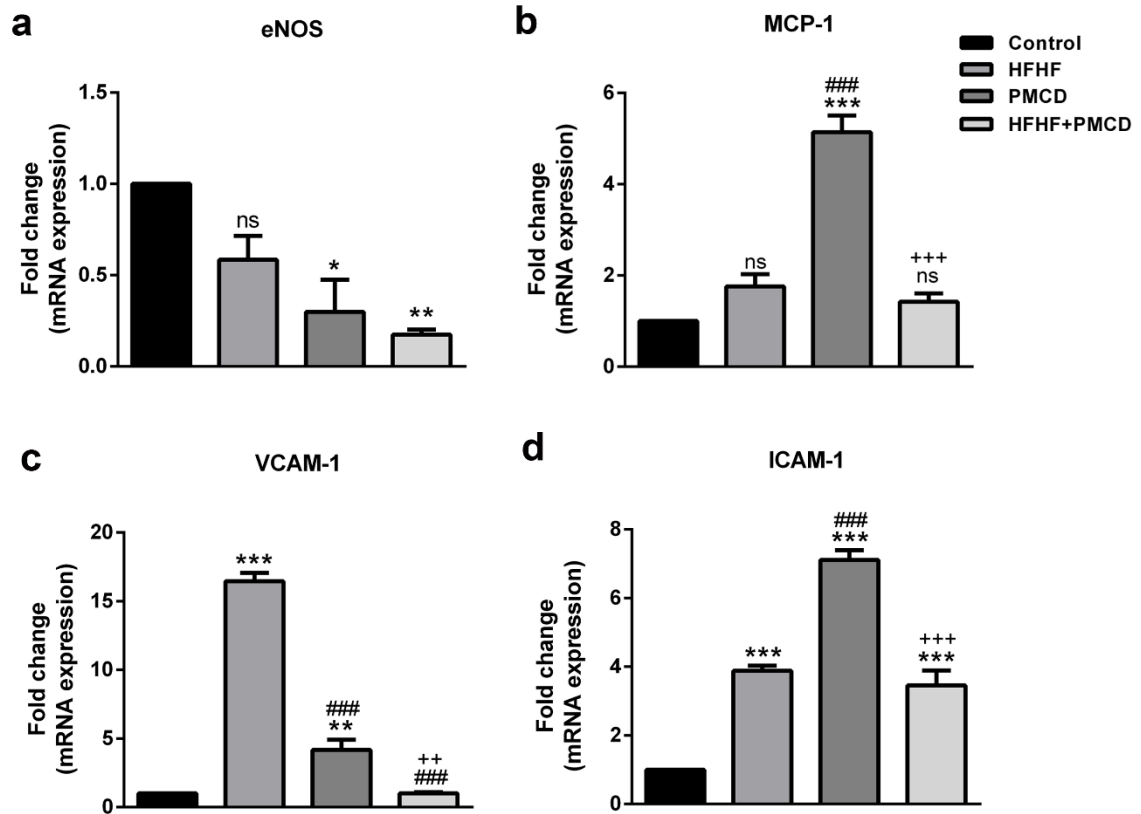


Figure 4.8: Endothelial dysfunction and activation in thoracic aorta. mRNA expression of (a) eNOS, (b) MCP-1, (c) VCAM-1 and (d) ICAM-1 in thoracic aorta were analyzed by quantitative RT-PCR. Data were expressed as Mean \pm SEM (n=3). * p <0.05, ** p <0.01, *** p <0.001 vs Control; ### p <0.001 vs HFHF; ++ p <0.01, +++ p <0.001 vs PMCD, ns- non-significant.

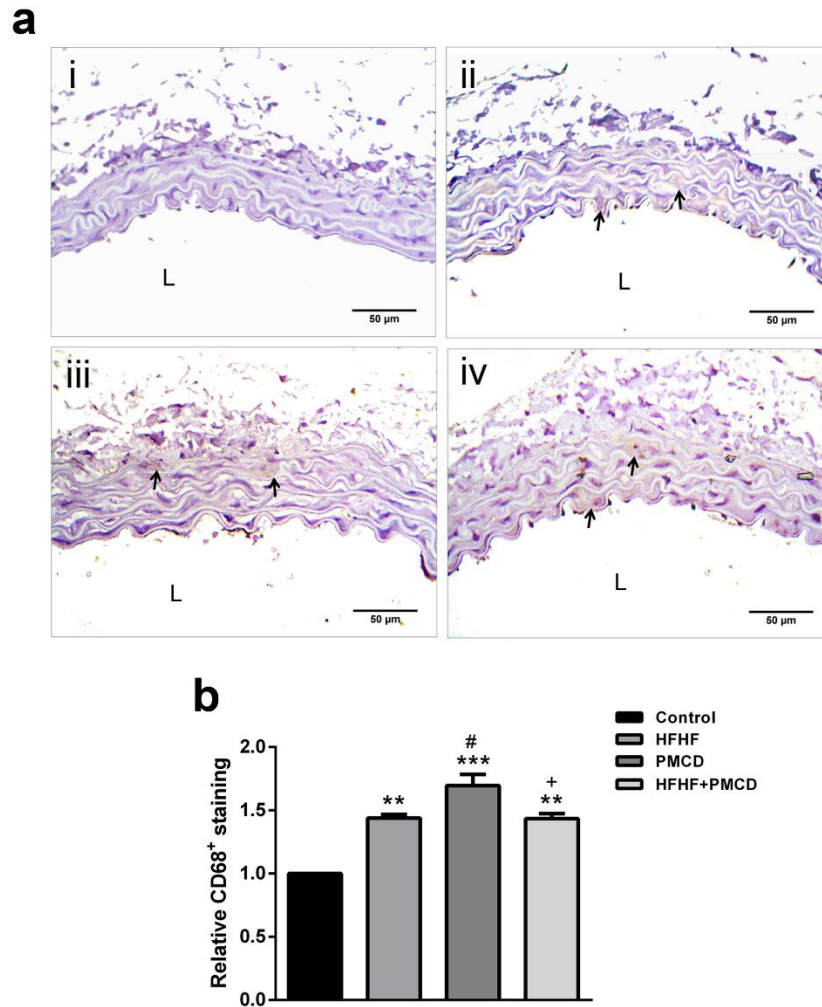


Figure 4.9: Macrophage infiltration in thoracic aorta. (a) Sections of thoracic aorta of i- Control, ii- HFHF, iii- PMCD, iv- HFHF+PMCD groups were immunostained for CD68 (Scale bar=50 μ m) where black arrows indicate positive stained regions. (b) Graph represents intensity of positive stained areas quantified using ImageJ. Data were expressed as Mean \pm SEM (n=6). **p<0.01, ***p<0.001 vs Control; #p<0.05 vs HFHF; +p<0.05, +++p<0.001 vs PMCD. L-Lumen.

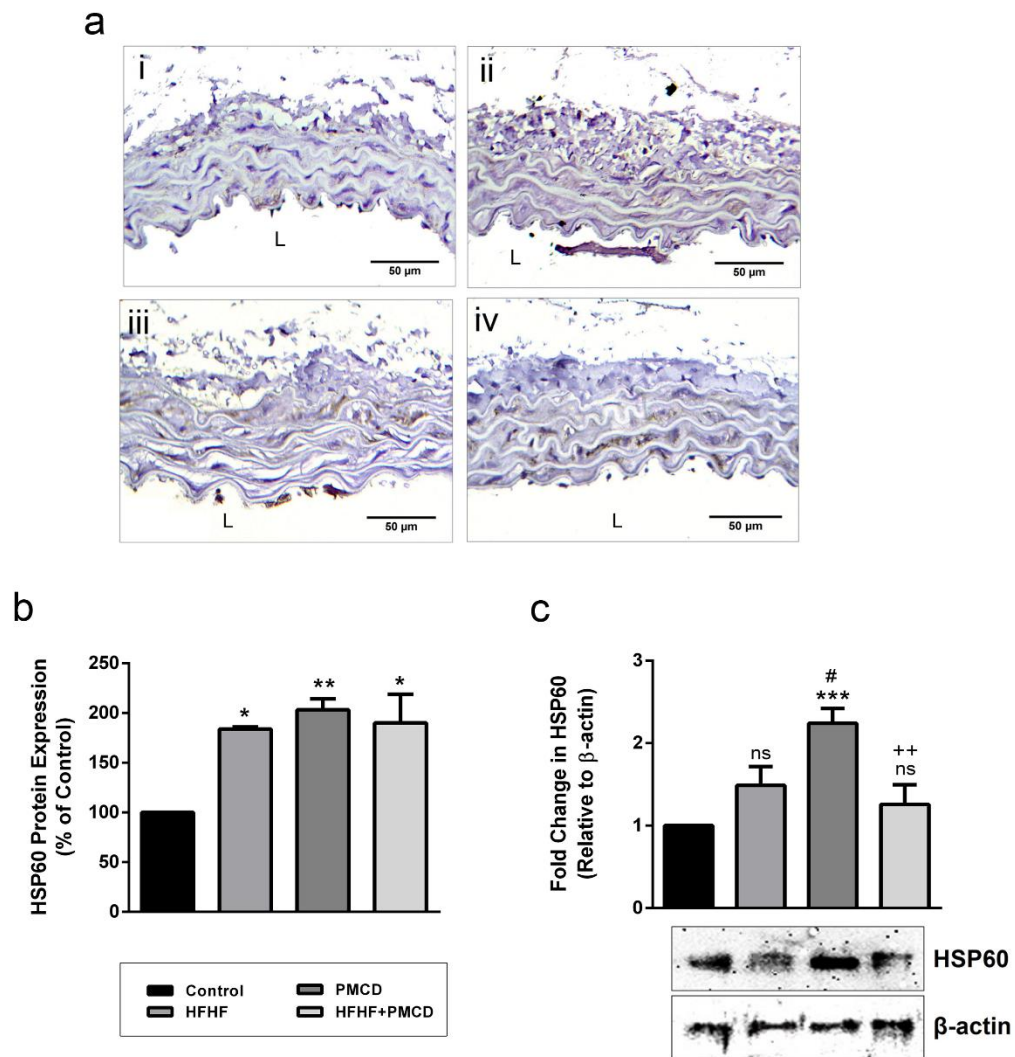


Figure 4.10: HSP60 expression in thoracic aorta. (a) Sections of thoracic aorta of i- Control, ii- HFHF, iii- PMCD, iv- HFHF+PMCD groups were immunostained for HSP60 and (b) positive stained regions were quantified using ImageJ (n=6). (c) HSP60 expression was checked by immunoblotting and the bands were quantified by densitometry (n=3). Data were represented as Mean ± SEM. *p<0.05, **p<0.01 vs Control; +p<0.05 vs PMCD, ns- non-significant. L-Lumen.

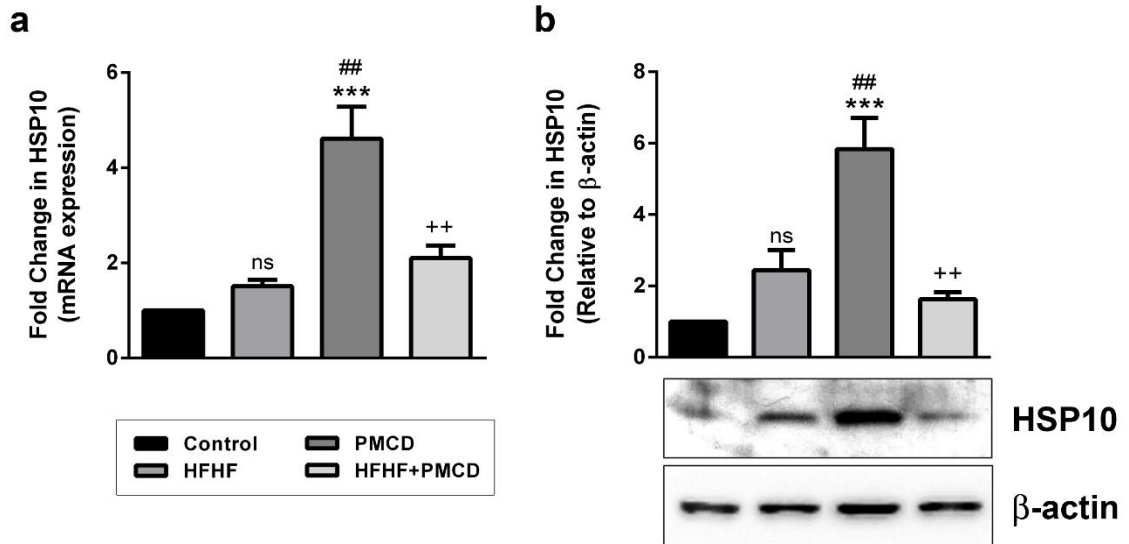


Figure 4.11: HSP10 expression in thoracic aorta. (a) mRNA expression of HSP10 was checked in thoracic aorta by quantitative RT-PCR and (b) its protein levels were checked immunoblotting followed by its densitometric quantification. Data were represented as Mean \pm SEM (n=3). ***p<0.001 vs Control; ###p<0.01 vs HFHF; ++p<0.01 vs PMCD, ns-non-significant.

Discussion

High fat diet and the resulting hyperlipidemia has been associated with atherogenic manifestations and the same is a widely used model for research in atherosclerosis. However, development of cardiovascular ailments in conditions of normolipidemia has been described and evidences have highlighted HSP60 as a pathogenic mediator in these circumstances. Dysregulation of circadian rhythm has been associated with impairment of various physiological processes that form the basis of a range of metabolic diseases but, the atherogenic consequences have not been investigated with respect to normolipidemic physiology. In the present study, pro-atherogenic changes in thoracic aorta resulting due to photoperiodic manipulation induced chronodisruption in C57BL/6J mice fed with laboratory chow were investigated and the results have been compared with healthy (Control) and HFHF diet fed mice (HFHF). Further, HFHF diet fed mice subjected to circadian deregulation (HFHF+PMCD) has also been investigated for atherogenic pathophysiology.

The results of lipid profile revealed that HFHF has a dominance in HFHF+PMCD group as the overall serum profiles were found to be comparable in both the groups. However, the prominent features in lipid profile of PMCD group were the significant increment in TG and VLDL, and significant decrement in HDL-Chol. Physiological relevance of HDL-Chol is well-established in lipid homeostasis where it constitutes an inevitable component of reverse cholesterol transport (Kinoshita et al., 2004). Herein, the observed low levels of HDL-Chol accounts for the pro-atherogenic changes in PMCD group as the levels of TC and LDL-Chol did not record significant increment. A cross-sectional study conducted in Sweden had correlated shift work with increased triglycerides and decreased HDL-

Cholesterol levels in human subjects (Karlsson et al., 2001) and our results of PMCD group complied with these reports.

Studies with mice and rat models fed with atherogenic diet and high fat diet have shown elevated lipid profiles and associated atherogenic changes of varying degrees in thoracic aorta (Cai et al., 2005; Santana et al., 2014). Also, our laboratory had previously reported atherogenic diet induced derangement in thoracic media and intima layers in rat model (Jadeja et al., 2012; Patel et al., 2013; Thounaojam et al., 2012). In Chapter 1, we had observed similar changes of increased IMT and lumen area in HFHF fed mice. In the present study, feeding with HFHF diet with or without exposure to PMCD showed hypertrophic remodeling of the thoracic aorta that marks the early stages of atherosclerosis in hyperlipidemic condition. Interestingly, we report pro-atherogenic remodeling of higher degree in thoracic aorta of mice subjected to experimentally induced chronodisruption and laboratory chow diet feeding. Further, disorganization of elastin lamellae along with increased collagen deposition explains the higher collagen-to-elastin ratio indicating towards arterial stiffening and a loss of vascular tone in HFHF, PMCD and HFHF+PMCD groups. The overall structural derangement of thoracic aorta observed herein, implies towards a functional loss that was surprisingly more prominent in mice subjected to PMCD group. Also, the pro-atherogenic vascular remodeling observed in thoracic aorta of PMCD group is a significant finding because these mice were fed with laboratory chow diet. Photoperiodic alterations induced aggravation of atherosclerosis in ApoE*3-Leiden.CETP mice has been reported wherein, the mice fed were maintained on a Western type diet. Another study by Anea et al. (2009) had reported pro-atherogenic vascular remodeling in Bmal1 knockout and Clock mutant mice maintained in constant darkness but these mice

were also naturally hyperlipidemic. In this regard, our results provide first evidence on the role of photoperiodic manipulation induced chronodisruption as a causative agent for atherosclerosis without feeding atherogenic/high fat diet.

At this point, atherogenic transformation of endothelium was clearly demonstrated by decrement in eNOS and increment in MCP-1, VCAM-1 and ICAM-1 that confirmed endothelial dysfunction and activation in all the three experimental conditions. These set of observations are in agreement with reports on high fat diet/ atherogenic diet mediated induction of atherosclerosis (Jadeja et al., 2012; Lang et al., 2019; Thounaojam et al., 2012). Further, increased staining of CD68 (macrophage marker) indicated towards increased macrophage infiltration in the vascular wall that is crucial event subsequent to endothelial damage during atherogenic progression. ApoE*3-Lesion.CETP mice subjected to photoperiodic alterations had showed augmented monocyte recruitment in lesions but, diet induced hyperlipidemia was not ruled out as a contributing factor (Schilperoort et al., 2020). Herein, the aggravated response observed in PMCD group in terms of macrophage infiltration further supports the atherogenic progression in light of photoperiodic manipulation induced chronodisruption even in absence of dietary atherogenic stimuli.

Expression of adhesion molecules has been associated with HSP60 upregulation in atherogenic vascular endothelial cells and the same has been functionally correlated in chapter 2 wherein, HSP60 overexpression induced upregulation of adhesion molecules in endothelial cells was observed. Herein, we report HSP60 upregulation in thoracic aorta of all the three experimental conditions with comparable levels in HFHF and HFHF+PMCD groups and significantly higher levels in PMCD group. Since, atherogenic manifestations as well as HSP60 upregulation was more prominent in mice subjected to PMCD, the two

events can be said to be functionally related. HSP60 upregulation suggests elevated levels of physiological stress in thoracic aorta (Hochleitner et al., 2000) as reported in smokers and hypertensive patients without conditions of hypercholesterolemia (Almanzar et al., 2012). Herein, we hypothesize that the pro-atherogenic changes observed in PMCD mice in spite of near normal levels of TC and LDL-Chol are attributable to photoperiodic alteration mediated physiological stress and upregulation of HSP60 in thoracic aorta coupled with significantly low levels of HDL-Chol.

Considering the HSP10 upregulation observed in thoracic aorta and HUVEC stressed with HFHF and OxLDL, respectively (chapter 1 & 2), it was imperative to study the same in conditions of normolipidemia. Herein, we observed upregulation of HSP10 in thoracic aorta in all the three experimental groups with maximum indices in PMCD group, adding to the evidences of atherogenic relevance of HSP10. Upregulation of HSP10 in conditions of normolipidemic atherosclerosis is an interesting observation that goes together with HSP60 alterations. However, detailed investigation of the underlying regulatory mechanisms and specific role of HSP10 in atherogenic events needs further investigation.

Taken together, our study highlights the role of HSP60 in inducing PMCD mediated pro-atherogenic changes wherein, near normal levels of LDL-Chol and decrement in HDL-Chol are significant observations. Herein, we also conclude that a combination of HFHF and PMCD (HFHF+PMCD) does not result in synergistic symptoms. Altogether, the findings hint at a possible underlying mechanism of atherosclerosis in normolipidemic patients with HSP60 at the epicenter.